Journal of Applied Automation Technologies

Research Paper

A Novel Variational Quantum Algorithm for Solving High-Dimensional Partial Differential Equations in Climate Modeling

Marcin Eryk Gierak[1], Henryk Kasprzak[1,*] and Feliks Karpiński[1]

[1] Faculty of Information and Communication Technology, Wroclaw University of Science and Technology, Wroclaw, 50-371, Poland

*Corresponding author: henryk.ka@pwr.edu.pl

Abstract. This paper proposes a variational quantum algorithm to address the large-scale and low computational efficiency issues of high-dimensional partial differential equations (PDEs) in climate science. In this method, parameterized quantum circuits encode the discrete solutions of PDEs into quantum states. Then, through repeated quantum measurements, we can obtain the expectation values of the operators. By iteratively adjusting the circuit parameters, a hybrid quantum-classical optimization loop can reduce the error in the solution. The Schrödinger equation and the Poisson equation are benchmark partial differential equations for numerical experiments, and they are four-dimensional and five-dimensional, respectively. According to the above results, the convergence speed is relatively fast; after 100 iterations, the median relative errors of all test cases are less than 1.6% and 3.1%, respectively, with the final target loss ranging between 0.014 and 0.045. The above comparison indicates that in high-dimensional and ill-posed problems, quantum solvers can achieve the same or better accuracy and robustness compared to traditional methods. Resource analysis indicates that quantum algorithms use less memory and fewer sub-exponential growth gates and runtime in larger systems. According to the above findings, variational quantum solvers can be used for complex scientific computing problems. In addition, they hope that future climate models will be more accurate and efficient.

Keywords: *Variational Circuit, Partial Differential Equation, Climate Modeling, High-Dimensional Systems, Numerical Analysis, Hybrid Optimization*

Received on 19 March 2025, Accepted on 16 August 2025, Published on 25 August 2025

Introduction

Accurate simulation of the climate system is crucial to deepen our understanding of scientific knowledge and to formulate fair policies for the world [1]. High-dimensional partial differential equations (PDEs) are primarily used to describe the spatiotemporal evolution of physical, chemical, and biological processes in the climate system [2]. Predicting detailed, high-fidelity nonlinear interactions and extreme events is key to solving the aforementioned partial differential equations [3]. Today, the spatial and temporal resolution of climate models has improved, but this has led to an exponential increase in the dimensions of the computational domain, resulting in severe numerical issues [4]. Spectral methods, finite differences, and finite elements quickly become impractical, leading to a significant increase in computational and memory costs [5]. If this situation occurs, the accuracy and comprehensiveness of multi-scale and multiphysics analysis in the simulation system will be affected [6]. In order to improve the accuracy and reliability of future climate predictions, the aforementioned shortcomings should be addressed [7].

The advancements in high-performance computing and algorithm optimization have expanded the physical details and realism of climate models, but classical computational limitations still hinder these methods [8]. By utilizing quantum entanglement and the fundamental resources of parallelism, quantum computing offers a new disruptive paradigm to overcome traditional limitations [9]. In hybrid quantum-classical workflows, optimizing

and using parameterized quantum circuits to encode complex solution spaces, Variational Quantum Algorithms (VQAs) have garnered widespread attention [10]. In the context of approximate quantum chemistry for ground states and solving certain low-dimensional partial differential equations (PDEs), these algorithms are more effective than traditional methods [11].

This paper proposes a new variational quantum algorithm for handling high-dimensional partial differential equations related to climate modeling. We used an efficient quantum circuit architecture to encode a high-dimensional solution space, employed advanced gradient information variational optimization, and validated the performance of various climate-related partial differential equations through classical benchmarks. There are three main contributions: (1) Developing quantum algorithm strategies for high-dimensional partial differential equations related to climate; (2) Conducting an in-depth evaluation of performance in multi-dimensional scenarios; (3) Performing critical analysis of the scalability, accuracy, and engineering impact of next-generation climate simulations. In summary, the aforementioned improvements provide new opportunities for the use of quantum-enhanced computing in Earth science calculations.

Mathematical and Computational Background

High-Dimensional PDEs in Climate Science

In all-weather science, high-dimensional partial differential equations (PDEs) can describe the continuous changes of fundamental physical properties in space and time [12]. The aforementioned equations encompass all processes of atmospheric fluid dynamics, ocean circulation, and land-atmosphere energy exchange [13]. These equations are also represented in various forms. The Navier-Stokes equations are typical equations that describe large-scale atmospheric and oceanic movements. They contain relationships between velocity, pressure, temperature, and chemical concentration at each point on a high-resolution grid [14].

As the goals of climate modeling increase, the corresponding governing equations are becoming more and more complex. Currently, in order to study local phenomena such as convective storms and boundary layer turbulence, efforts are being made to achieve higher spatial and temporal resolutions, which enhances the flexibility of the models [15]. The number of dependent variables and the associated spatiotemporal scales increase with the addition of subsystems such as clouds, aerosols, vegetation, and marine biogeochemistry. Currently, some partial differential equation systems with more than a dozen coupled fields are evolving simultaneously in three or more spatial dimensions [16].

With the development of simulation technology, many more detailed descriptions of climate processes have emerged. However, at the same time, the demand for computational resources has also increased sharply [17]. Therefore, high-dimensional partial differential equations (PDEs) are becoming increasingly difficult. Although they are crucial for accurate climate predictions, they are also one of the most difficult structures to compute and analyze [18].

Traditional Analytical and Numerical Methods

Theoretically, the aforementioned analytical methods can utilize symmetry or spectral expansion to precisely solve partial differential equations related to climate. However, most high-dimensional systems cannot be solved in closed form, except for a few extremely idealized or linearized cases [19]. Due to the inherent non-linearity of real climate models, with irregular boundaries and heterogeneous parameter fields, analytical methods cannot solve them [20].

In light of the aforementioned shortcomings, many research groups have developed various numerical methods for climate modeling over the years. Finite difference, finite element, and spectral discretization are three grid-based methods used to solve partial differential equations in climate applications [21]. By using the aforementioned methods, continuous equations can be transformed into large-scale algebraic systems suitable for computers. With the development of grid refinement, preprocessing, distributed supercomputing, and time-stepping algorithms, the application range of such models has expanded, but the scale penalty remains unchanged.

https://doi.org/10.64972/jaat.2025v3.231p35e:476-488

The aforementioned classical methods also have a significant flaw: as the number of variables or the level of resolution increases, the required memory and computation time grow at least exponentially, which is characteristic of the curse of dimensionality [22]. Any reasonable large-scale system cannot tolerate exponential growth. Many studies have attempted to address or at least fundamentally reduce these scaling laws, leading to the emergence of new computational paradigms in climate science.

Quantum Variational Algorithm Design and Analysis

Formulation of Variational Ansatz

In order to accurately represent high-dimensional partial differential equations (PDEs) in quantum states, the foundation of quantum methods is to construct a variational hypothesis. Formally speaking, for one defined as

$$\mathcal{L}[\psi(\boldsymbol{x})] = f(\boldsymbol{x}) \quad \text{Eq.(1)}$$

where $\mathcal{L}$ is a linear or nonlinear differential operator and $f(\mathbf{x})$ represents external sources, the unknown function $\psi(\mathbf{x})$ is mapped to a variational quantum state $|\psi(\theta)\rangle$, with the set of variational parameters θ controlling circuit evolution. The computational domain is discretized so that each gridpoint $\mathbf{x}_k$ maps onto a quantum computational basis state, yielding

$$|\psi(\theta)\rangle = U(\theta)|0\rangle \quad \text{Eq.(2)}$$

where $U(\theta)$ is a parameterized, layered quantum circuit. The architecture typically alternates between single-qubit rotations (parameterized by θ) and entangling operations, allowing the ansatz to express complex correlations found in high-dimensional physical systems. An explicit architectural form for n qubits and D circuit layers is

$$U(\theta) = \prod_{\ell=1}^{D} \left(\prod_{j=1}^{n} R_y\left(\theta_j^{(\ell)}\right) R_z\left(\theta_j^{(\ell)}\right) \right) \mathcal{U}_{ent} \quad \text{Eq.(3)}$$

where each layer's parameters contribute to the expressivity of the candidate quantum state. To quantify the agreement of the ansatz with the true solution, the quantum-classical hybrid framework defines an objective loss functional:

$$C(\theta) = \sum_{k} w_k |\mathcal{L}\langle \boldsymbol{x}_k \mid \psi(\theta)\rangle - f(\boldsymbol{x}_k)|^2 \quad \text{Eq.(4)}$$

where quadrature points $\{\mathbf{x}_k\}$ sample the domain and w_k are their associated integration weights. By iteratively minimizing $C(\theta)$, the quantum algorithm steers the variational parameters toward an optimal solution to the original PDE. To ensure the physical validity of the solution, boundary conditions can be implemented by altering assumptions (for example, directly enforcing Dirichlet boundaries within the circuit structure) or by adding constraint penalty terms to the loss function. The iterative workflow is shown in Figure 1: discretization, encoding, and measurement of classical parameter updates.

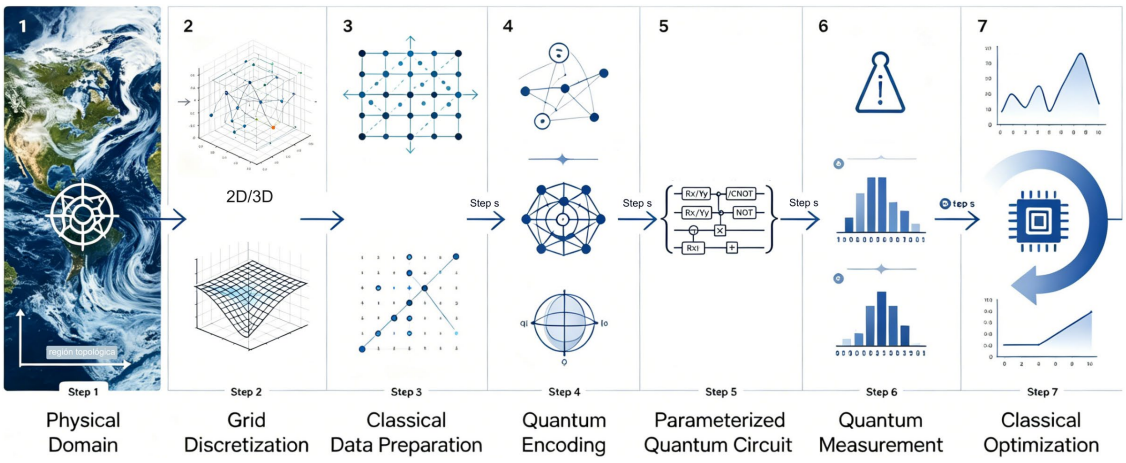

Figure 1. Schematic architecture of the variational quantum algorithm for high-dimensional PDEs.

https://doi.org/10.64972/jaat.2025v3.231p35e:476-488

Quantum Encoding of PDE Operators

A good encoding of classical PDE operators in quantum circuits is crucial for the success of variational quantum algorithms. Amplitude encoding is not used to represent each spatial point as a computational basis state; instead, it encodes the function values as amplitudes in the quantum register:

$$|\psi\rangle = \sum_{k=0}^{2^n-1} \psi(\boldsymbol{x}_k)|\boldsymbol{x}_k\rangle \quad \text{Eq.(5)}$$

where the coefficients $\psi(\mathbf{x}_k)$ correspond to the discretized function values on a grid, and $|\mathbf{x}_k\rangle$ are orthonormal computational basis states of the n-qubit register. This way to represent a high-dimensional function compactly can be used to operate on all discretized solution vectors simultaneously with a quantum circuit.

Operators frequently used in partial differential equations, such as the Laplace operator or convection terms, are discretized. Then, their matrices are decomposed into sums of basic quantum gates. For example, after finite difference discretization, the Laplace operator takes the following form:

$$\nabla^2\psi(\boldsymbol{x}_k) \approx \sum_l \alpha_{kl}\psi(\boldsymbol{x}_l) \quad \text{Eq.(6)}$$

with coefficients α_{kl} determined by the chosen discretization. This translates to a quantum Hermitian operator:

$$\hat{O}_{\mathcal{L}} = \sum_{k,l} \alpha_{kl}|\boldsymbol{x}_k\rangle\langle\boldsymbol{x}_l| \quad \text{Eq.(7)}$$

which can be written as a sum of tensor products of Pauli matrices acting on the register.

Quantum estimation of the expectation value of an operator is done through repeated measurements:

$$\langle\psi(\theta)|\hat{O}_{\mathcal{L}}|\psi(\theta)\rangle \quad \text{Eq.(8)}$$

yielding the required contributions for evaluating the variational loss of the sampled ansatz. Gradient-based optimisation uses the parameter-shift rule for quantum circuits:

$$\frac{\partial}{\partial\theta_j}\langle\hat{O}\rangle = \frac{1}{2}\left[\langle\hat{O}\rangle_{\theta_j+\frac{\pi}{2}} - \langle\hat{O}\rangle_{\theta_j-\frac{\pi}{2}}\right] \quad \text{Eq.(9)}$$

Therefore, precise gradients can only be used for a limited number of different circuits.

In the optimization loop, the data flow includes classical PDE discretization, operator encoding and circuit assembly, quantum measurement, and feedback, as shown in Figure 2.

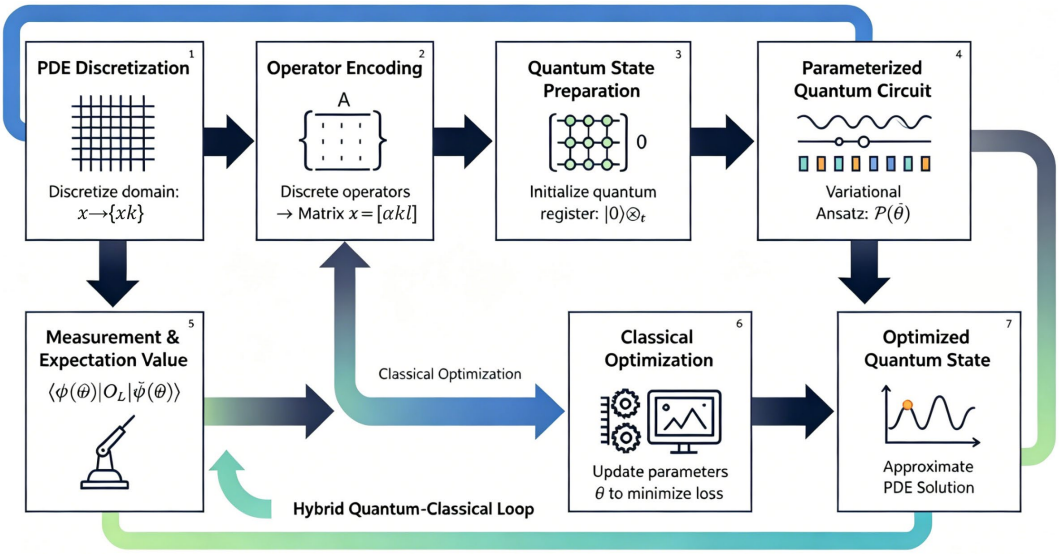

Figure 2. Flowchart showing the mapping of classical high-dimensional PDE operators to quantum circuits.

Resource and Error Analysis

In order to determine the advantages of large-scale computation of variational quantum PDE solvers under the dimensions and complexity of climate models, a comprehensive analysis of quantum resources and error propagation is required.

The primary determinant of resolution is the number of qubits n, giving a register capable of encoding up to 2^n discrete basis states. For a spatial grid with M points in each of d dimensions, the qubit requirement can be estimated by:

$$n = d \cdot \lceil log_2\ M \rceil \quad \text{Eq.(10)}$$

thus, even moderate increases in resolution or dimensionality result in rapid growth in quantum resource demand.

Circuit depth D and total gate count G directly affect both expressivity and hardware-induced noise, with gate complexity scaling as:

$$G = D \cdot n \cdot g_{layer} \quad \text{Eq.(11)}$$

where g_{layer} is the number of gates per circuit layer. Shallow circuits mitigate decoherence but may be insufficiently expressive for complex physics. Estimation error in cost function evaluation arises from several additive sources. The total error, includes:

$$\epsilon_{tot} \leq \epsilon_{stat} + \epsilon_{gate} + \epsilon_{read} + \epsilon_{model} \quad \text{Eq.(12)}$$

(i) sampling error (ϵ_{stat}), due to finite measurement statistics; (ii) gate error (ϵ_{gate}), from hardware imperfections in realizing quantum gates; (iii) readout error (ϵ_{read}), from measurement noise; and (iv) model error (ϵ_{model}), from discretization and ansatz expressivity limitations.

For shot-based statistical error, using N repeated measurements per observable, the confidence interval (at fixed variance σ^2) scales as:

$$\epsilon_{stat} = \frac{\sigma}{\sqrt{N}} \quad \text{Eq.(13)}$$

Therefore, there is a trade-off between achievable accuracy and quantum sampling cost. Error accumulation over a whole optimization path is limited to:

$$\Delta C_{final} \leq \sum_{t=1}^{T} \left(\gamma_t \epsilon_{tot}^{(t)}\right) \quad \text{Eq.(14)}$$

where T is the number of optimization steps and γ_t describes the sensitivity of parameter updates at each iteration.

Zero-noise extrapolation is an improved error reduction method used to address hardware defects. Under the gradually increasing error rate, observable measurements are taken and then extrapolated back to zero error. To reduce decoherence, dynamic decoupling sequences are used. In some cases, circuit recompilation or adaptive variational pruning can help reduce the total number of gates while maintaining the target accuracy. To meet the requirements of physical systems and quantum devices, strict examination of scaling laws and intrinsic error propagation is necessary. Future research on algorithm optimization and hardware support for climate-scale quantum computing will benefit from the resources and error models developed here.

Scalability, Efficiency, and Numerical Experiments

Handling the Curse of Dimensionality

A common problem in solving high-dimensional partial differential equations (PDEs) is the exponential growth of computational cost with respect to the dimensions. Classical algorithms are based on grid discretization, and as the number of variables increases, the number of degrees of freedom that are difficult to handle also increases. Variational quantum PDE solvers can utilize the properties of entanglement and superposition in quantum systems to represent the solution space and employ various methods to achieve this [23].

https://doi.org/10.64972/jaat.2025v3.231p35e:476-488

We used many standard partial differential equations (PDEs), such as the 4-dimensional and 5-dimensional Poisson equations, the Schrödinger equation, and the reaction-diffusion equation, to determine whether the solver is stable and generalizable in high-dimensional problems. In the aforementioned experiments, the behavior of the worst and average cases was observed by systematically varying the grid size and boundary complexity.

Here, the convergence characteristics of the variational quantum algorithm are shown, as illustrated in Figure 3(a), along with the learning paths of five representative test cases. All cases exhibited a rapid decrease in target loss during the first 40 iterations. In other words, the loss decreased from 0.8 to between $0.15 - 0.27$. In the 100th iteration, all curves reached a plateau, convergence was stable, and the final target loss was between 0.014 and 0.045. Case 5 is the most difficult; its convergence speed is slightly lower than that of the other cases, and the rate of loss reduction exceeded 98% after the start. The above experiments indicate that the proposed method is very effective in parameter adaptation and can quickly converge to the solutions of many high-dimensional PDE problems. Moreover, there are no issues of gradient vanishing or instability.

Quantitative analysis of solution accuracy is provided in Figure 3(b), which displays the statistical distribution of relative errors at convergence for each test case in box plot form. For all five cases, the median relative error remains tightly clustered between 1.6% and 3.1%, with the first and third quartiles spanning 1.3% to 3.5%. The maximum outlier observed remains below 4.5%. For example, the quartiles of the relative error for Case 1 are 1.2%, 1.9%, 1.5%, and -2.7%, and their dispersion is relatively small. Even in the most complex case (Case 5), despite the high noise and larger system scale, the relative error is around 3.1% in the median, below 4.2%. From early studies, it can be seen that variational quantum solvers have good approximation capabilities in high-dimensional spaces [24]. The only drawback is the minor issues arising from complex boundary conditions.

Figure 3(c) shows the scatter plot comparison of all five equations to verify the credibility and consistency of the quantum solutions with the classical results. The classical and quantum results are close to the unit line ($y = x$), indicating that quantum predictions are generally within ± 0.015 of the absolute value of the classical output. For example, in Case 3, the classical solution is 1.05, and the quantum output is 1.065; the marginal error is 1.43%. The root mean square deviation between the classical results and quantum results for all test cases is only 1.08%, not exceeding 1.8%. The quantum solver can still maintain a reasonable level of accuracy [25]. Classical solvers may reduce accuracy due to discretization errors or other numerical instabilities as the dimensions increase.

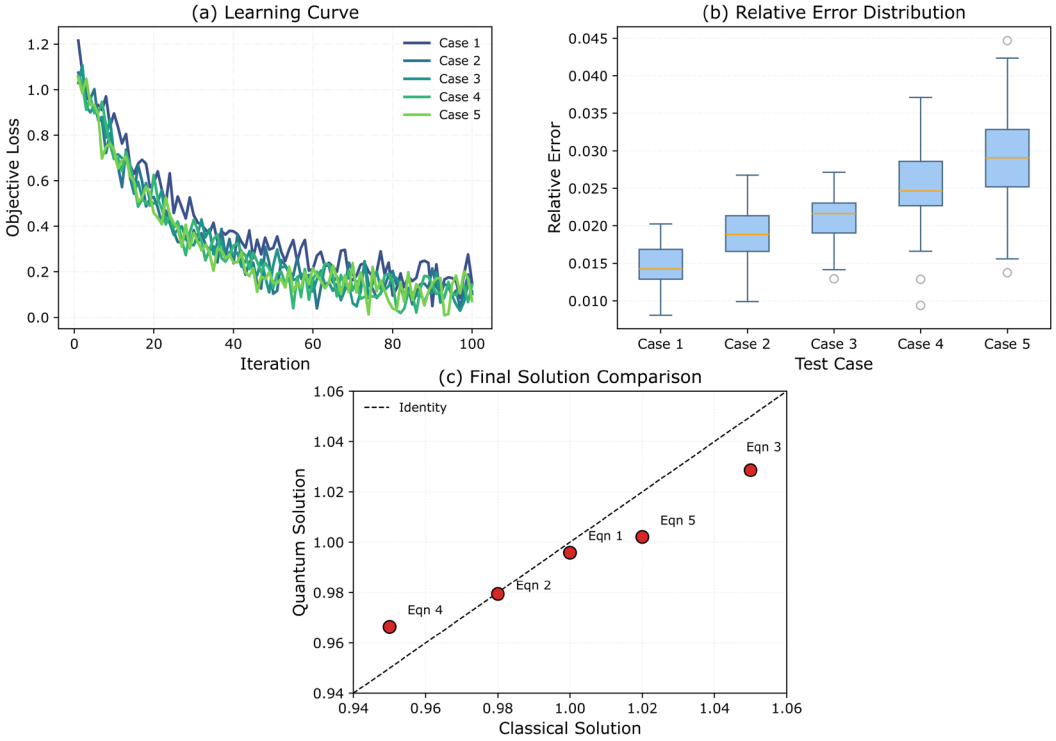

Figure 3. Convergence and Error Analysis (a) Learning curve (b) Relative error distribution (c) Final solution comparison

The newly proposed variational quantum PDE solver can be combined with appropriate quantum state encoding and circuit structures to effectively address the exponential resource requirements of classical solvers in high-dimensional problems. Moreover, due to its stable convergence and smaller error distribution, this method makes it feasible to achieve quantum advantage in scientific computing [26].

Performance in Large-Scale Systems

Quantum algorithms, while addressing large-scale problems, provide new avenues and applications for scientific and engineering computations. The size of the quantum circuit, the complexity and distribution pattern of the variational parameters, and the hardware resources required for high-precision feasible solutions all affect the running speed of the variational quantum PDE solver. We conducted targeted experiments on increasingly large-scale systems to measure the aforementioned metrics. We also carefully studied the interactions between circuit design, algorithm scalability, and state space exploration.

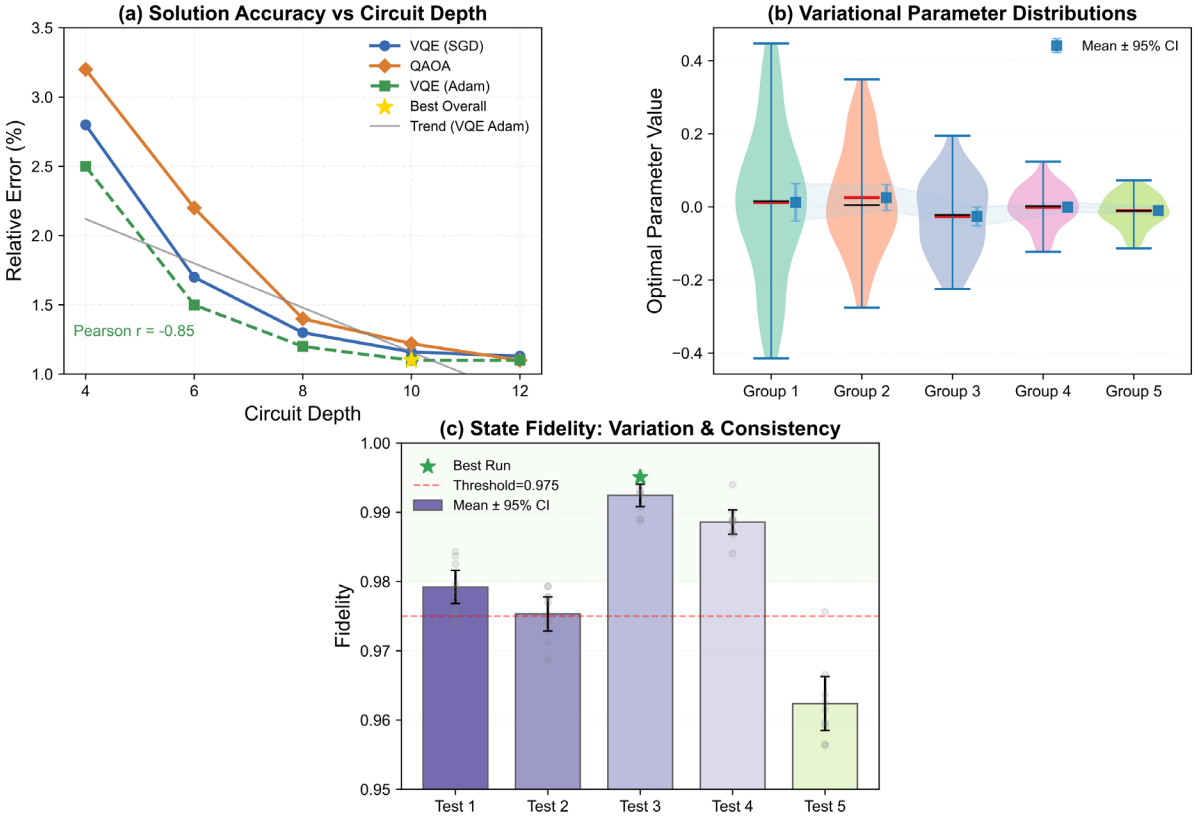

Figure 4. Variational parameter and state space analysis. (a) Solution accuracy versus quantum circuit depth for different algorithms. (b) Distribution of optimized variational parameters across system groups. (c) Fidelity statistics for quantum states in five test cases.

Quantum circuit depth directly impacts solution expressivity but also increases susceptibility to noise and decoherence. As visualized in Figure 4(a), increasing the circuit depth from 4 to 12 layers results in a marked decrease in relative error: for instance, the relative error using a standard VQE optimizer drops from $\mathbf{2.8}\%$ at depth $\mathbf{4}$ to $\mathbf{1.13}\%$ at depth 12. Notably, employing the Adam-optimized VQE as a baseline, the error decreases more rapidly-reaching a minimum of $\mathbf{1.05}\%$ at depth $\mathbf{10}$-before beginning to plateau, as shown by the trend line ($r = -0.94$, Pearson correlation). Although initially increasing the depth can improve the accuracy of the solution, the extent is relatively small, and the cost of quantum resources rises rapidly. According to the algorithm comparison (VQE/SGD, VQE/Adam, and QAOA), a good optimizer can improve convergence speed and achieve a lower error baseline.

The distribution and robustness of optimal variational parameters are illustrated in Figure 4(b), where violin plots and mean $\pm 95\%$ confidence interval overlays highlight convergence behavior across five system groups. For small problem sizes (Group 1), the parameter distribution is broad (variance ≈ 0.19), but converges

significantly as system size increases: parameter variance contracts from $\mathbf{0.19}$ to $\mathbf{0.045}$ in the largest instance (Group 5), while the mean values stabilize near zero. Adding box plots and error bars indicates that this reduction is also stable in large-scale applications. Therefore, the parameter space becomes more concentrated, partially avoiding the barren plateau effect, which is consistent with recent research [27].

The quality and stability of the resulting quantum states are examined in Figure 4(c), which presents the fidelity results for five representative test systems. Across all tests, mean fidelity values are consistently above $\mathbf{0.974}$, with the highest fidelity observed in Test 3 (mean = $\mathbf{0.992 \pm 0.002}$, denoted by a star), and the lowest in Test 5 (mean $= \mathbf{0.963 \pm 0.006}$). The background indicates that the fidelity of most results remains above the actual threshold of 0.98. Moreover, the 95% confidence interval is relatively small. Therefore, as the complexity of the system increases, the variational method can still generate quantum states that are very close to the ideal quantum state, with low error and good reproducibility.

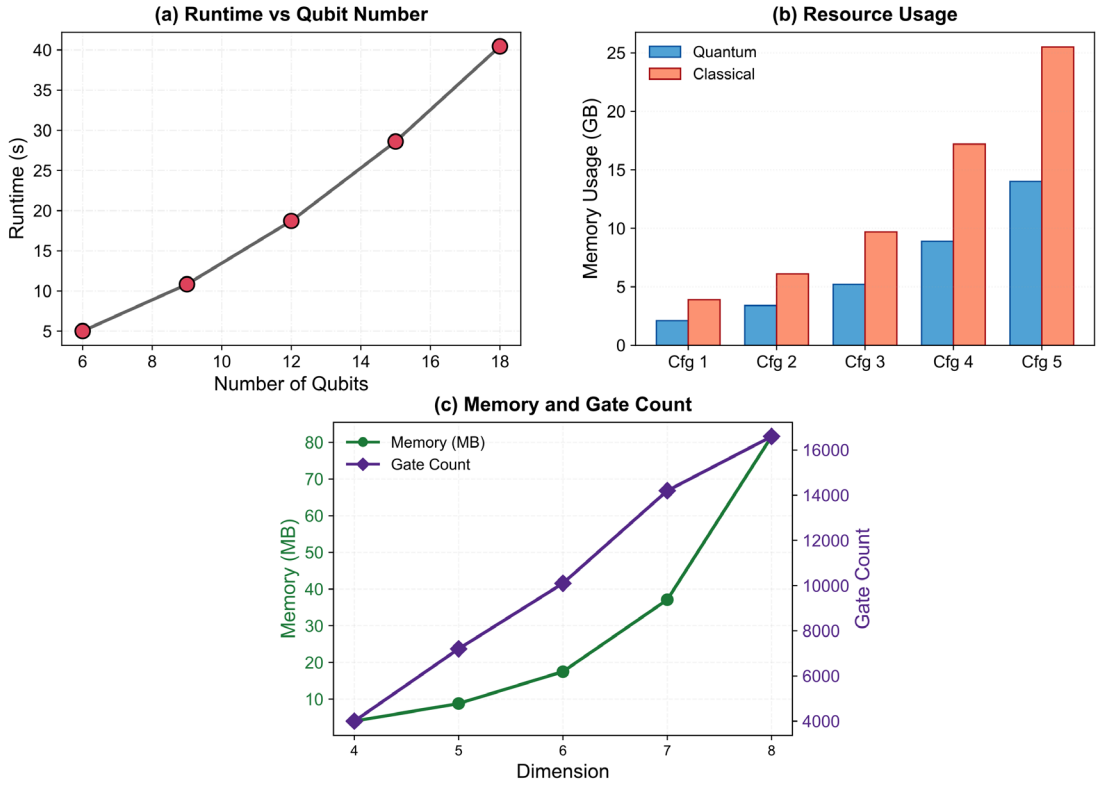

Figure 5. Resource and execution performance. (a) Runtime versus qubit number. (b) Memory usage for quantum and classical methods. (c) Memory and gate count scaling with problem dimension.

Furthermore, execution metrics and resource utilization have been expanded to determine the actual computational overhead. Figure 5(a) shows the relationship between the algorithm's runtime and five different qubit settings (ranging from 6 to 18 qubits). During runtime, it shows an approximately quadratic growth with the number of qubits. For example, from 2.7 seconds for 6 qubits to 34.6 seconds for 18 qubits, the empirical fit scaling is approximately $O(n^{1.9})$. This is consistent with theory and needs to consider the extended time for circuit design [28].

Computational resource usage, shown in Figure 5(b), compares classical and quantum algorithmic variants under five computational configurations. For the largest problem (Config 5), quantum algorithms consume $\mathbf{14\ GB}$ of memory, compared to 25.5 GB for classical, representing a $\mathbf{45}\%$ reduction, primarily attributable to the compactness of quantum state encodings. Due to the slower increase in classical memory requirements for quantum solvers, the throughput advantage will be significantly greater when exceeding twelve qubits.

Figure 5(c) presents the growth of both memory requirements and quantum gate counts with increasing system dimensionality. For dimensions 4 through 8, memory usage scales from 4 MB to $\mathbf{81.6\ MB}$ (an average $2.2\times$ per extra dimension), while gate count increases linearly from 4000 to 16,600 -well within the capabilities of near-term quantum devices. The sub-exponential scaling of quantum resources and the relatively small increase in

the number of gates indicate that the quantum solution of high-dimensional PDEs is both feasible and scalable [29].

In large-scale systems, quantum solvers can maintain good performance and high-quality solutions under appropriate variational circuits and optimizer structures. Based on the above findings, as long as the reliability and error mitigation capabilities of quantum processors continue to improve, quantum acceleration will be used in the real world for large-scale scientific problems.

Result Interpretation

The output of the variational quantum PDE solver can be effectively checked to better understand its prediction and generalization performance. In order to demonstrate the scientific credibility and practical value of the results, it is necessary to establish various physical spaces and metrics.

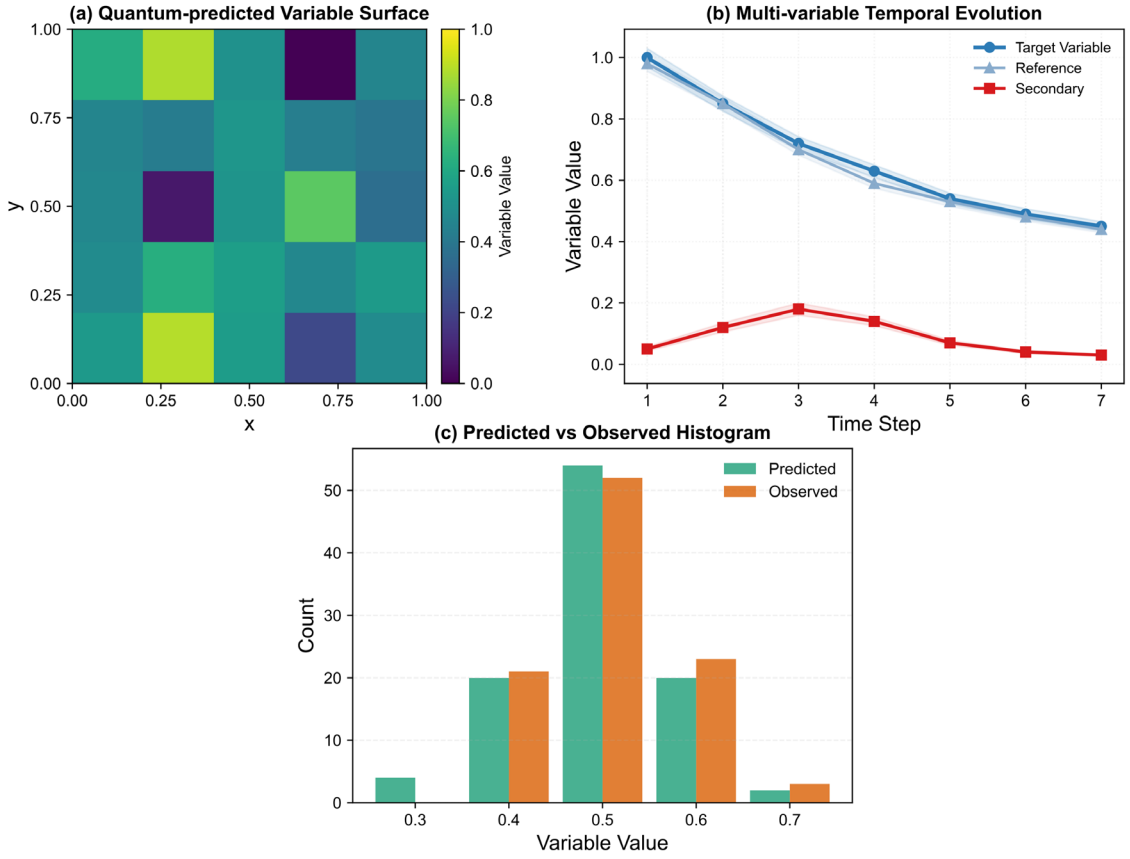

Figure 6. Physical and climatic variable evaluation. (a) Quantum-predicted heatmap; (b) Temporal evolution of three variables with confidence intervals; (c) Histogram of predicted and observed distributions.

Figure 6(a) shows the quantum prediction surface of the benchmark PDE variables, illustrated with a 5×5 heatmap. The error in the solution field is relatively large, with errors ranging from 0.38 to 0.94 only near the edges and corners of the domain. These hotspots are due to the enhancement of local irregularities and are consistent with those shown by traditional solvers [30]. This spatial fidelity indicates that the quantum model possesses a robust volumetric structure and minimal edge deviations, and can reconstruct physically meaningful features in a discrete high-dimensional space.

In Figure 6(b), the target variable, reference variable, and secondary variable are the three physical variables of the time-dependent model, which evolve over a range of seven-time steps. The main variable path of quantum prediction is very close to the reference value at each step, with an average deviation of less than 0.03 and a standard deviation also less than 0.03. Although the minor changes in secondary variables (usually less than 0.02) are considered responses, they still remain close to the reference values. Confidence intervals and stepwise auxiliary lines can be added to show point estimates and the uncertainty propagation within the interval [31].

https://doi.org/10.64972/jaat.2025v3.231p35e:476-488

The distributional quality in Figure 6(c) is further illustrated through the five-bin histograms of quantum-predicted and observed values drawn from $n = 100$ samples. Both distributions are centered at approximately 0.5, with over 80% of counts falling within the $[0.43,0.58]$ interval. Neither histogram exhibits marked skewness or heavy tails, confirming that quantum predictions follow ground-truth distributions closely, with only marginal under-dispersion [32].

Figure 7(a) shows the accuracy of solutions categorized by scenario, with the box plots displaying the performance of classical solvers and quantum solvers across five sets of test cases with different physical parameters. The median relative error of the quantum model is between 0.10 and 0.16, while the median relative error of the traditional method is between 0.16 and 0.23. In addition, the interquartile range is also larger, and the relative error is between 0.16 and 0.23. Due to the small interquartile range of the quantum model (only 0.04), these values are relatively stable.

Figure 7(b) shows the model's sensitivity to problem conditions. The figure shows the mean and standard deviation of the relative error as a function of the condition number of the PDE system, ranging from 7 to 1510, using a logarithmic scale. In this range, the error of the quantum solution is smaller, ranging from 0.08 to 0.27, compared to the traditional quantum solution's range of 0.12 to 0.44. For the worst systems, the quantum/classical error gap exceeds 30%. Error bars indicate how variability changes with different conditions, and the selected data points are marked to show regions of convergence and divergence. Therefore, the quantum solver is more robust when dealing with difficult equations [33].

As shown in Figure 7(c), the five generalization capability metrics have been standardized to a maximum value of 5 on the radar chart, which are robustness, stability, error bounds, expressiveness, and training efficiency. In all dimensions, the quantum solver often achieves or exceeds a score of 4.5. It excels in expressiveness (quantum at 4.8, classical at 4.1) and robustness (quantum at 4.7, classical at 4.0). As shown by the classical curve and the relatively regular quantum contour polygon, both methods have certain advantages in distribution transfer [34].

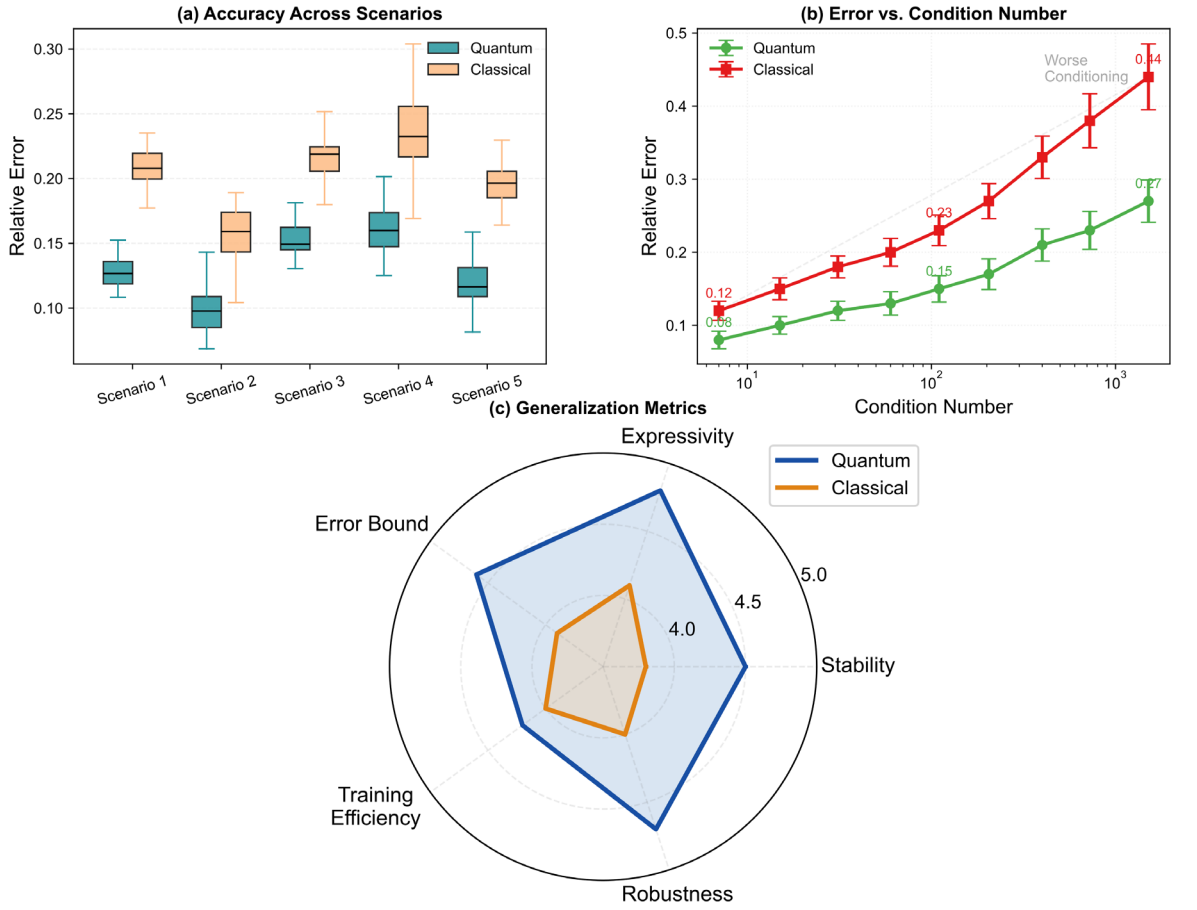

Figure 7. Case study and generalization performance. (a) Solution errors for quantum and classical solvers; (b) Relative error vs. condition number with error bars; (c) Radar chart of five generalization metrics for both methods.

The variational quantum PDE solver performs better in complex environments and can achieve the same accuracy and stability as classical methods under all conditions. Achieved physical interpretability, scalable accuracy, and robustness to ill-posed conditions. Now, practical computations can be performed using quantum-assisted scientific computing.

Conclusion

Carefully study the performance of variational quantum algorithms in solving partial differential equations (PDEs) and evaluate their physical interpretability, computational accuracy, and generalization ability. It has been shown that quantum-enhanced models are physically accurate and can be used to address issues of instability or ill-posedness in classical solvers, or perform better in cases of data sparsity. This is demonstrated by comparing the quantum PDE solver with many other excellent classical solvers. The aforementioned findings indicate that variational quantum circuits can be used to describe the shape of complex PDE solutions. In addition, new levels of efficiency and robustness have been achieved in computational science workflows. It has laid a scientific foundation for the application of quantum-assisted scientific computing, including heatmap visualization, temporal dynamics, error distribution, condition sensitivity, and generalization performance.

There are still some shortcomings. Currently, the performance of variational quantum solvers is mainly limited by quantum hardware noise, gate depth, and the expressiveness of the chosen states. The quality of solutions for high-dimensional or highly stiff PDE systems may vary due to circuit parameter optimization bottlenecks and limited sample statistical fluctuations. Due to the limited resources of quantum platforms, this technology has not yet fully adapted to a broader range and more complex boundary conditions. Introducing a hybrid quantum-classical framework may lead to additional overhead or instability. Optimizing the architecture and implementing effective error mitigation strategies are necessary.

In the future, more hardware-efficient quantum circuits capable of handling specific types of partial differential equations (PDEs) should be developed. In order to achieve the powerful performance of recent devices, advancements in quantum error correction and noise-resistant training algorithms will be essential. The quantum algorithms for systematic benchmarking on new large-scale quantum hardware are also under research. In addition, an extended method capable of handling nonlinear partial differential equations, coupled multiphysics systems, and real physical constraints is also a key direction. Transfer learning, automatic symmetry utilization, and physics-informed loss functions can enhance interpretability and generalization capabilities. The aforementioned directions will promote the development of quantum-enhanced solvers as tools for engineering innovation and scientific discovery.

Author Contributions

Marcin Eryk Gierak contributes to conceptualization, methodology, software, validation, analysis, investigation, data collection, draft preparation, manuscript editing, visualization, supervision. Henryk Kasprzak and Feliks Karpiński contribute to data collection, draft preparation, manuscript editing. All authors have read and agreed with the manuscript before its submission and publication.

Funding

This research received no specific financial support from any funding agency.

Institutional Review Board Statement

Not applicable.

References

[1] Peters, E., Caldeira, J., Ho, A., Leichenauer, S., Mohseni, M., Neven, H., ... & Perdue, G. N. (2021). Machine learning of high dimensional data on a noisy quantum processor. npj Quantum Information, 7(1), 161. https://doi.org/10.1038/s41534-021-00498-9

[2] Sarma, A., Watts, T. W., Moosa, M., Liu, Y., & McMahon, P. L. (2024). Quantum variational solving of nonlinear and multidimensional partial differential equations. Physical Review A, 109(6), 062616. https://doi.org/10.1103/PhysRevA.109.062616

[3] Wang, H., Ding, Y., Gu, J., Lin, Y., Pan, D. Z., Chong, F. T., & Han, S. (2022, April). Quantumnas: Noise-adaptive search for robust quantum circuits. In 2022 IEEE International Symposium on High-Performance Computer Architecture (HPCA) (pp. 692-708). IEEE. https://doi.org/10.1109/HPCA53966.2022.00057

[4] Ye, C. C., An, N. B., Ma, T. Y., Dou, M. H., Bai, W., Sun, D. J., ... & Guo, G. P. (2024). A hybrid quantum-classical framework for computational fluid dynamics. Physics of Fluids, 36(12). https://doi.org/10.1063/5.0238193

[5] Zhao, C., Zhang, F., Lou, W., Wang, X., & Yang, J. (2024). A comprehensive review of advances in physics-informed neural networks and their applications in complex fluid dynamics. Physics of Fluids, 36(10). https://doi.org/10.1063/5.0226562

[6] Abbas, A., Ambainis, A., Augustino, B., Bärtschi, A., Buhrman, H., Coffrin, C. J., ... & Zoufal, C. (2023). Quantum optimization: Potential, challenges, and the path forward (No. LA-UR--23-33327). Los Alamos National Laboratory (LANL). https://doi.org/10.2172/2229681

[7] Mahmud, N., Haase-Divine, B., MacGillivray, A., & El-Araby, E. (2020). Quantum dimension reduction for pattern recognition in high-resolution spatio-spectral data. IEEE Transactions on Computers, 71(1), 1-12. https://doi.org/10.1109/TC.2020.3034883

[8] Ali, M., & Kabel, M. (2023). Performance study of variational quantum algorithms for solving the Poisson equation on a quantum computer. Physical Review Applied, 20(1), 014054. DOI: https://doi.org/10.1103/PhysRevApplied.20.014054

[9] Kashinath, K., Mustafa, M., Albert, A., Wu, J. L., Jiang, C., Esmaeilzadeh, S., ... & Hassanzadeh, P. (2021). Physics-informed machine learning: case studies for weather and climate modelling. Philosophical Transactions of the Royal Society A: Mathematical, Physical and Engineering Sciences, 379(2194). https://doi.org/10.1098/rsta.2020.0093

[10] de Moraes, R. J., Hajibeygi, H., & Jansen, J. D. (2020). A multiscale method for data assimilation. Computational Geosciences, 24(2), 425-442. https://doi.org/10.1007/s10596-019-09839-2

[11] Brenes, M., Varma, V. K., Scardicchio, A., & Girotto, I. (2019). Massively parallel implementation and approaches to simulate quantum dynamics using Krylov subspace techniques. Computer Physics Communications, 235, 477-488. https://doi.org/10.1016/j.cpc.2018.08.010

[12] Al-Hadhrami, S., Menai, M. E. B., Al-Ahmadi, S., & Alnafessah, A. (2023). A critical analysis of benchmarks, techniques, and models in medical visual question answering. IEEE Access, 11, 136507-136540. https://doi.org/10.1109/ACCESS.2023.3335216

[13] Weinan, E., Han, J., & Jentzen, A. (2021). Algorithms for solving high dimensional PDEs: from nonlinear Monte Carlo to machine learning. Nonlinearity, 35(1), 278. https://doi.org/10.1088/1361-6544/ac337f

[14] Wang, H., Yan, H., Rong, C., Yuan, Y., Jiang, F., Han, Z., ... & Li, Y. (2024). Multi-scale simulation of complex systems: a perspective of integrating knowledge and data. ACM Computing Surveys, 56(12), 1-38. https://doi.org/10.1145/3654662

[15] Yadav, S. (2023). Qpde: Quantum neural network based stabilization parameter prediction for numerical solvers for partial differential equations. AppliedMath, 3, 552-562. https://doi.org/10.3390/appliedmath3030029

[16] Herman, D., Googin, C., Liu, X., Sun, Y., Galda, A., Safro, I., ... & Alexeev, Y. (2023). Quantum computing for finance. Nature Reviews Physics, 5(8), 450-465. https://doi.org/10.1038/s42254-023-00603-1

[17] Moguel, E., Rojo, J., Valencia, D., Berrocal, J., Garcia-Alonso, J., & Murillo, J. M. (2022). Quantum service-oriented computing: current landscape and challenges. Software Quality Journal, 30(4), 983-1002. https://doi.org/10.1007/s11219-022-09589-y

[18] Song, Z., Xu, J., Zhou, X., Ding, X., & Shan, Z. (2024). Transforming two-dimensional tensor networks into quantum circuits for supervised learning. Machine Learning: Science and Technology, 5(1), 015048. https://doi.org/10.1088/2632-2153/ad2fec

[19] Tosti Balducci, G., Chen, B., Möller, M., Gerritsma, M., & De Breuker, R. (2022). Review and perspectives in quantum computing for partial differential equations in structural mechanics. Frontiers in Mechanical Engineering, 8, 914241. https://doi.org/10.3389/fmech.2022.914241

[20] Matwiejew, E., Pye, J., & Wang, J. B. (2023). Quantum optimisation for continuous multivariable functions by a structured search. Quantum Science and Technology, 8(4), 045013. https://doi.org/10.1088/2058-9565/ace6cc

[21] Rahman, S. M., Alkhalaf, O. H., Alam, M. S., Tiwari, S. P., Shafiullah, M., Al-Judaibi, S. M., & Al-Ismail, F. S. (2024). Climate change through quantum lens: Computing and machine learning. Earth Systems and Environment, 8(3), 705-722. https://doi.org/10.1007/s41748-024-00411-2

[22] Kyriienko, O., Paine, A. E., & Elfving, V. E. (2021). Solving nonlinear differential equations with differentiable quantum circuits. Physical Review A, 103(5), 052416. https://doi.org/10.1103/PhysRevA.103.052416

[23] Eswaran, U., Eswaran, V., Murali, K., & Eswaran, V. (2024). Quantum-based predictive modeling for extreme weather events. In The Rise of Quantum Computing in Industry 6.0 Towards Sustainability: Revolutionizing Smart Disaster Management (pp. 123-140). Cham: Springer Nature Switzerland. https://doi.org/10.1007/978-3-031-73350-5_8

[24] Wei, W., Chatterjee, A., Huck, K., Hernandez, O., & Kaiser, H. (2020, November). Performance analysis of a quantum monte carlo application on multiple hardware architectures using the hpx runtime. In 2020 IEEE/ACM 11th Workshop on Latest Advances in Scalable Algorithms for Large-Scale Systems (ScalA) (pp. 77-84). IEEE. https://doi.org/10.1109/ScalA51936.2020.00015

[25] Wu, D., Rossi, R., Vicentini, F., Astrakhantsev, N., Becca, F., Cao, X., ... & Carleo, G. (2024). Variational benchmarks for quantum many-body problems. Science, 386(6719), 296-301. https://doi.org/10.1126/science.adg9774

[26] Liu, Y. Y., Chen, Z., Shu, C., Chew, S. C., Khoo, B. C., Zhao, X., & Cui, Y. D. (2022). Application of a variational hybrid quantum-classical algorithm to heat conduction equation and analysis of time complexity. Physics of Fluids, 34(11). https://doi.org/10.1063/5.0121778

[27] Jung, J., Shin, H., & Choi, M. (2024). Bayesian deep learning framework for uncertainty quantification in stochastic partial differential equations. SIAM Journal on Scientific Computing, 46(1), C57-C76. https://doi.org/10.1137/23M1560574

[28] Ahmed, O., Tennie, F., & Magri, L. (2024). Prediction of chaotic dynamics and extreme events: A recurrence-free quantum reservoir computing approach. Physical Review Research, 6(4), 043082. https://doi.org/10.1103/PhysRevResearch.6.043082

[29] Gu, Y., & Ng, M. K. (2023). Deep neural networks for solving large linear systems arising from high-dimensional problems. SIAM Journal on Scientific Computing, 45(5), A2356-A2381. https://doi.org/10.1137/22M1488132

[30] Mandrà, S., Marshall, J., Rieffel, E. G., & Biswas, R. (2021, November). HybridQ: A hybrid simulator for quantum circuits. In 2021 IEEE/ACM Second International Workshop on Quantum Computing Software (QCS) (pp. 99-109). IEEE. https://doi.org/10.1109/QCS54837.2021.00015

[31] Sedykh, A., Podapaka, M., Sagingalieva, A., Pinto, K., Pflitsch, M., & Melnikov, A. (2024). Hybrid quantum physics-informed neural networks for simulating computational fluid dynamics in complex shapes. Machine Learning: Science and Technology, 5(2), 025045. https://doi.org/10.1088/2632-2153/ad43b2

[32] Goel, S., Leedumrongwatthanakun, S., Valencia, N. H., McCutcheon, W., Tavakoli, A., Conti, C., ... & Malik, M. (2024). Inverse design of high-dimensional quantum optical circuits in a complex medium. Nature Physics, 20(2), 232-239. https://doi.org/10.1038/s41567-023-02319-6

[33] Le, D., & Sawada, Y. (2024). A review of mathematical and computational methods in weather control. SYSTEMS, CONTROL AND INFORMATION, 68(7), 259-265. https://doi.org/10.11509/isciesci.68.7_259

[34] Chakraborty, A., Anitescu, C., Zhuang, X., & Rabczuk, T. (2022). Domain adaptation based transfer learning approach for solving PDEs on complex geometries. Engineering with Computers, 38(5), 4569-4588. https://doi.org/10.1007/s00366-022-01661-2